TESTS AND ANALYSIS OF A NOVEL SEGMENTATION METHOD USING MEASUREMENT DATA

Isabel MORENO
University of Cordoba – Spain
p92mogai@uco.es

Aurora GIL-de-CASTRO
University of Cordoba – Spain
agil@uco.es

Irene Y.H. GU
Chalmers – Sweden
irenegu@chalmers.se

Math BOLLEN
LTU – Sweden
math.bollen@ltu.se

ABSTRACT

Fault detection in power systems and its diagnosis are highly relevant issues within a power quality scope. Detailed analysis of disturbance recordings, like voltage dips, requires accurate segmentation methods. A joint causal and anti-causal (CaC) segmentation method has been introduced but only been tested with synthetic signals. In this paper, its performance has been analysed with a set of real measurement signals.

INTRODUCTION

In the process of transmission and distribution of energy from power plants to the end points of consumption that takes place through the power grids, the voltage waveform undergoes alterations that can impact certain users. The analysis of alterations in the voltage waveform has increasingly become a very important aspect, which has led to an increased interest in equipment that monitor the quality of electrical power. This premise leads to the concept power quality (PQ) [1]–[4], which is closely related to grid efficiency and electricity production.

Evaluating the electrical system disturbances involves study of deviations for the voltage and current from the ideal waveform. In general, these deviations can be classified into two groups under PQ paradigm: variations and events [1]. The former (eg, harmonics, overvoltages, unbalance, etc.) are generally regarded as small and gradual deviations from the sine wave voltage / current, characterized as steady-state phenomena; the latter occur producing sudden large deviations of the waveform, and are characterized as non-stationary random phenomena, usually caused by incidents in the operating conditions of the electrical system.

As well, automatic event detection and analysis in power systems and its diagnosis are highly relevant issues with PQ monitoring. According to [5], the first step in the gathering of information from a power quality event is the detection and subsequently segmentation, and analysis. This means that the first point where an event begins or ends is found and then the segmentation is performed to divide the event into parts. The detection and segmentation of event waveforms are related to finding both quasi-stationary parts and non-quasi-stationary parts of the signal at a given time scale. Usually event detection is an online process that leads to the activation record of the event, while the event segmentation is afterward performed, during the analysis of a recorded event.

A Kalman filter-based joint causal and anti-causal (CaC) segmentation method is introduced by [6]. The study suggests a statistically-based method to determine the threshold of detection parameter (DP) and a CaC method to locate boundary points between transition and event segments. The performance of the method has been quantified using synthetic voltage waveforms [6] but has not been applied by any author to large numbers of measured voltage waveforms. In this paper, CaC method is analyzed with several voltage-dip recordings obtained at different locations in medium voltage networks. The other main contribution of this paper is the use of cusum (cumulative sum) method as statistical estimator to determine the DP and the threshold.

METHODOLOGY

In this section, a modified version of CaC segmentation described by [6] is presented as an efficient solution to the correct identification of non-stationary and quasi-stationary stages in measured voltage waveforms. A total of one hundred recording files of dip events are available to this end, which are categorized according to the ABC classification [5]. These signals are events recorded by power quality instruments and contain both pre-trigger and post-trigger information.

To segment a waveform using CaC algorithm, the use of a statistical estimator is initially necessary to determine the threshold of the DP. Later the transition boundary segments are established according to the results of applying the segmentation using a causal analysis window plus an anti-causal analysis window.

Threshold Algorithm based on Cusum Theory

The following section shows how the statistical estimator used in this study works. The cusum algorithm is used to fast detect any abrupt change in the waveform. The basic principle of the algorithm is the incorporation of all the information from the sampled values. This is achieved by the cumulative sum of the deviations found in the sampling relative to a reference value (μ_0).

If the value of μ_0 is the ideal mean of the process control state (target value) and X_j is the average of the j^{th} sample, the cumulative sum method is given by (Eq.1):

$$C_i = \sum_{j=1}^{i}(X_j - \mu_0) \tag{1}$$

Where C_i is called cumulative sum up (including the i^{th} sample). Cusum determines that in any process on control state, the sum accumulated result of Eq.1 generates random values with mean zero. If the mean varies between two values processed in an increasing way, there will be a positive accumulation in C_i. On the other hand, if the mean processed varies in a decreasing way, there will be a negative accumulation in C_i. The combination of information from several samples makes the cusum a suitable method for detecting small changes in the process as well as on-line control.

The tabular cusum version [7] is designed to detect high and low changes in mean process, recording cumulative sums of the samples of a signal in two directions. For this reason, this method works by accumulating deviations from the mean that are above its ideal value with the parameter C^+ (upper cusum, Eq.2) and accumulating deviations from the mean that are below its ideal value with the parameter C^- (lower cusum, Eq.3):

$$C_i^+ = \max[0, x_i - (\mu_0 + K) + C_{i-1}^+ \tag{2}$$
$$C_i^- = \max[0, (\mu_0 - K) - x_i + C_{i-1}^-] \tag{3}$$

In Eq.2 and Eq.3, K is the reference value set with a value that allows a fast fault detection, which is usually half of the difference between the value of the average target control state and the value of the average in which the process is considered out of control. The process is considered to be out of control when any statistic crosses a decision interval (threshold H).

This method has been previously used to detect and classify disturbances on synthetic signals [8], [9]. In this case, several measured events have been tested. However, false alarms were generated in many cases. To set a threshold H that avoids false alarms, the cusum algorithm has been tested with all the files that were available and programming different values of K and H parameters. According to the data obtained, the method proposed to detect disturbances is only based on upper cusum C^+ (Eq.2) as statistical estimator to determine the DP and the threshold. This algorithm is configured as follows: K as 0.5 times the standard deviation of the filtered signal and H as 5 times the standard deviation of DP. The selection of the design parameter values (K, H) has a strong influence on the performance of the cusum algorithm.

To demonstrate this methodology, one phase of a type C dip (fast transition) is used. Fig. 1 shows an example based on the residual sequence from a high pass Butterworth filter (referred in the figure as filtered signal) and the statistical estimator positive cusum C^+ (referred to DP). Fig. 2 shows the disturbance detection of this dip. When the DP crosses H (the horizontal black line on Fig. 2(a), an indication flag (red square wave on Fig. 2(c)) is triggered. This flag is reset when DP falls below the threshold.

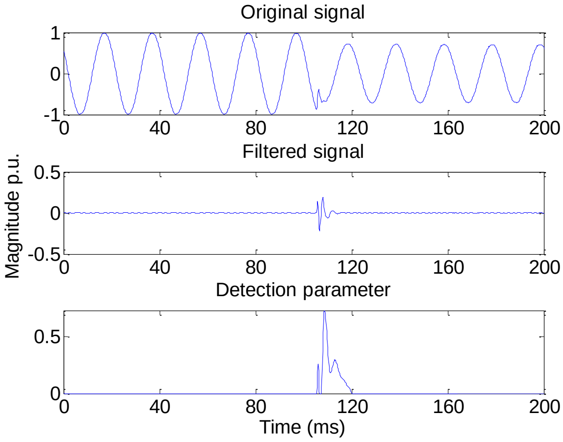

Fig. 1. From top to bottom: (a) Original signal; (b) Residual sequence from the Butterworth filter; (c) Resulting detection parameter (DP) obtained from (Eq.2).

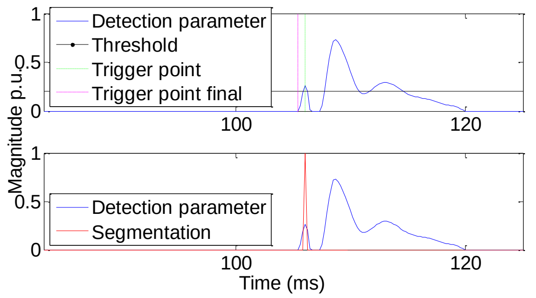

Fig. 2. (a) The DP with the established threshold and the trigger points (top); (b) Segmentation window (bottom).

To accurate estimate the first out of control instant of the process is, an additional parameter (N^+) must be considered. This parameter indicates the number of consecutive times that the DP has been nonzero after DP first crosses H. Finally, the non-stationary of the process is triggered as a result of subtracting N^+ to initially set trigger point.

From Fig. 2(a) one may see that the trigger point (the vertical dashed green line) is initially set in 106.04 ms, this time corresponds at the 509 sample. The out control variable (N^+) resulting from cusum is set to 3. Thus, the disturbance starts at the 506 sample. This sample corresponds to 105.41 ms (the vertical magenta green line).

Segmentation Algorithm based on CaC Theory

The CaC introduced by [6] consists in applying to a signal recorded of n samples a joint segmentation scheme using a causal (forward time, from zero to nth sample) plus an anti-causal (backward time, from nth to zero sample) analysis window. The purpose of this method is to obtain an accurate time allocation of the underlying transition based on the results from the two analysis window.

As said above, from a causal analysis window the out of control process point (causal flag) is obtained. On CaC, a similar process takes place in the opposite time direction and an anti-causal flag is also obtained. Combining these time instants, a causal and anti-causal flags, the transition is then allocated. In addition, the transition classification as slow or fast is possible by considering the position of the causal and anti-causal flags in relation to each other (Fig. 3).

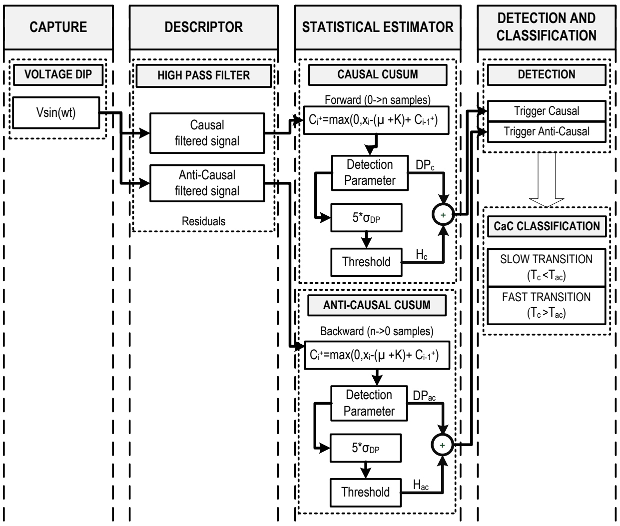

Fig. 3. Dip events detection and classification with the proposed method.

When there is an overlap between the two flags, the trigger time instant of causal flag is below the time instant of the anti-causal flag. In this case, the transition is considered to be slow and the estimated duration of the underlying transition is the duration of this overlap, defined by Eq.4:

$$\widehat{D}_0 = [T_{causal}, T_{anti-causal}] \qquad (4)$$

In the opposite case, if the trigger time instant of causal flag is above the trigger time instant of the anti-causal flag, then there is a gap between the two flags. The transition is considered to be fast and the time location of the underlying transition is estimated as the middle point of this gap, defined by Eq.5:

$$\widehat{T}_0 = (T_{causal} + T_{anti-causal})/2 \qquad (5)$$

To better describe the CaC segmentation, the disturbance shown in Fig 1(a) (fast transition) is used. First, the causal segmentation is applied to a disturbance sequence, using a sliding analysis window along the causal time direction. When the DP exceeds the threshold (or, the critical DP), a transition is detected for this window. The start of the transition is at sample 506 (105.41 ms).

Then, anti-causal segmentation is applied, where the analysis window now slides in the opposite direction (anti-causal time direction) to compute DP. Fig. 4 shows the anti-causal segmentation result, where the transition segment starts at sample 504 (105 ms). As causal and anti-causal segmentations give a detection delay, the actual trigger point of the transition segment is located between the two starting points from the causal and anti-causal segments. According to Eq.5, the detected trigger point of transition segment is at the (506+504)/2) = 505 (105.2 ms).

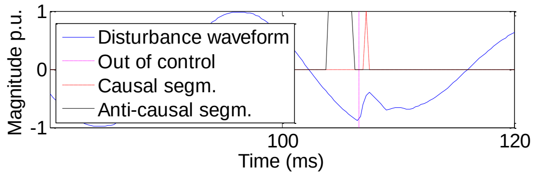

Fig. 4. Result from segmentation of the fast transition shown in Fig. 1(a).

RESULTS

The results presented correspond to measured signals that present dips with different type transitions: slow, fast and multi-stage transitions.

Slow transition

An example of a voltage dip due to a three-phase fault (or symmetrical fault) in a distribution system is shown in Fig. 5. In this case, there is the same voltage dip in the three phases. This is a typical type A dip [5].

Fig. 6 shows the CaC segmentation applied to the disturbance analyzed (zoomed in area around the transition segments). One can see that within the first segmentation shown in Fig. 6 (a) there are overlaps in the CaC flags in the three phases. The transition segment to a transition with overlap is considered as starting from the starting point of causal segment and ending at the starting point of anti-causal segment. The slow transitions for this segmentation have a duration of 24.37 ms for phase A (T_{causal}l = 101.04 ms and $T_{anti-causal}$ = 125.41 ms), 24.79 ms for phase B (T_{causal}l = 101.04 ms and $T_{anti-causal}$ = 125.83 ms) and 10 ms for phase C (T_{causal}l = 100.2 ms and $T_{anti-causal}$ = 110.2 ms). In the second segmentation shown in Fig. 6 (b), there are slow transitions for phases B (T_{causal}l = 1593.33 ms and $T_{anti-causal}$ = 1600.41 ms) and C (T_{causal}l = 1595 ms and $T_{anti-causal}$ = 1598.75 ms) but fast transition on phase A (1598.22 ms). These result that both detected CaC transitions areas are quite long.

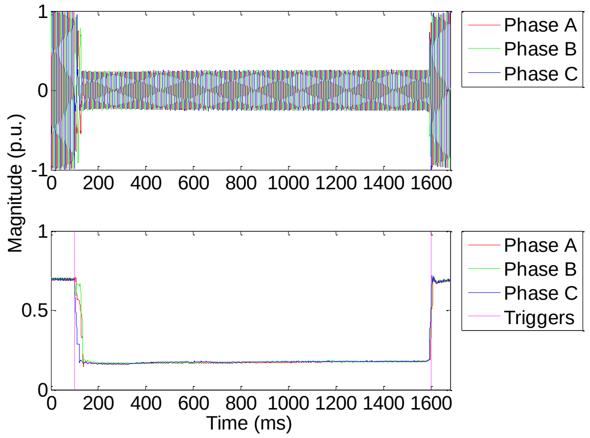

Fig. 5. Slow dip: (a) Voltages waveforms; (b) rms voltages and CaC segmentation.

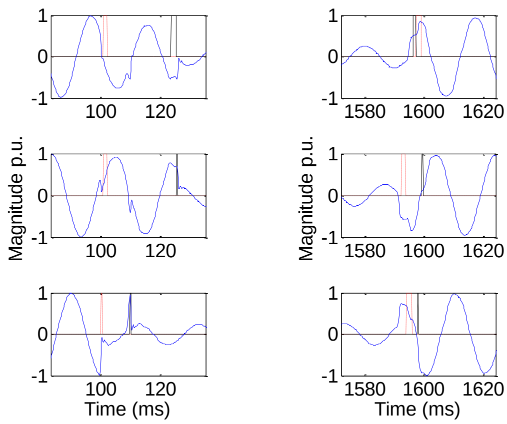

Fig. 6. Results from casual segmentation (dashed red line) and anti-causal segmentation (black line) for the slow dip shown in Fig. 5 (blue line): (a) First CaC segmentation (left); (b) Second segmentation (right).

Fast transition

An extreme case of a nonbalanced dip with an additional phase-angle jump is studied in Fig. 7. In this case the dip shows a large drop in phases A and C, however almost no drop in the phase B. These conditions are typical of a type C dip [5].

Fig. 8 shows the CaC segmentation applied to the disturbance studied (zoomed area around the transition segments). The first segmentation shown in Fig. 8(a) indicates a fault inception between phase A and phase C, phase B is not involved. There is no overlap for phase A, T_{causal} = 96.48 and $T_{anti-causal}$ = 93.12 ms. According to Eq.5, the detected trigger point of transition segment for phase A is at 94.79 ms. There is overlap in the CaC flags for phase C (T_{causal} = 94.79 ms and $T_{anti-causal}$ = 95 ms). The transition for phase C is found to start somewhere at before 94.79 ms. The second segmentation shown in Fig. 8(b) indicates that on recovery dip the phase B is involved. There is no overlap for phases ABC (fast transitions). The trigger points for phases ABC are 428 ms, 432 ms and 429 ms respectively. These result that both detected CaC transitions areas are quite short.

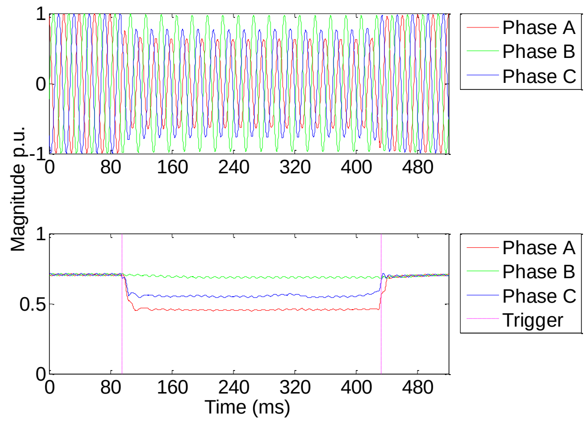

Fig. 7. Fast dip: (a) Voltages waveforms; (b) rms voltages and CaC segmentation.

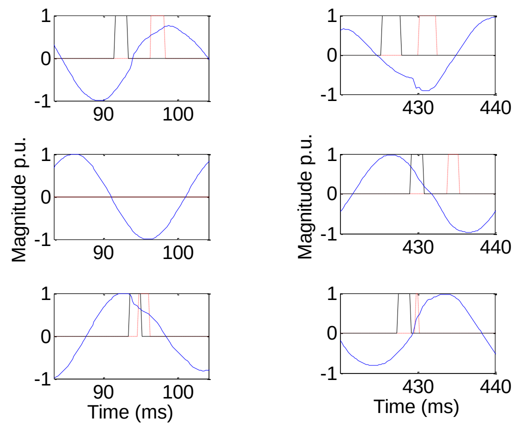

Fig. 8. Results from casual segmentation (dashed red line) and anti-causal segmentation (black line) for the fast dip shown in Fig. 7 (blue line): (a) First CaC segmentation (left); (b) Second segmentation (right).

Multi-stage transition

Fig. 9 shows a voltage dip due to a fault that develops from a single phase through two phases to ground to three phases [5].

Fig. 10 shows the CaC segmentation applied to the disturbance analyzed. The first segmentation indicates the start of a type D dip. This segmentation is characterized by fast transitions on two phases. According to Eq.5, the trigger points for phases A and B are 92.08 ms and 90.41 ms respectively. The second segmentation indicates that the dip develops into a type F dip, the transition is triggered in 294.16 ms for phase A and in 294.79 ms for phase C. This result that the development from a fast recovery dip to a slow recovery dip is fast. The third segmentation indicates a deviation on the dip. The two latest segmentations indicate the start and the end of a type A event. In the start of this event is detected by fast transitions in phase B (567.91 ms) and phase C (566.45 ms). This result that the development from a two phases to ground dip to a three phases dip the transition is fast. The last segmentation implies the type A event recovery. There are overlaps in the CaC flags for phase A (T_{causal} = 613.75 ms and $T_{anti-causal}$ = 617.5 ms) and phase B (T_{causa}l = 611.66 ms and $T_{anti-causal}$ = 616.45 ms). The recovery is triggered in phase C by a fast transition on 615. 41 ms. One can see that the recovery is quite long.

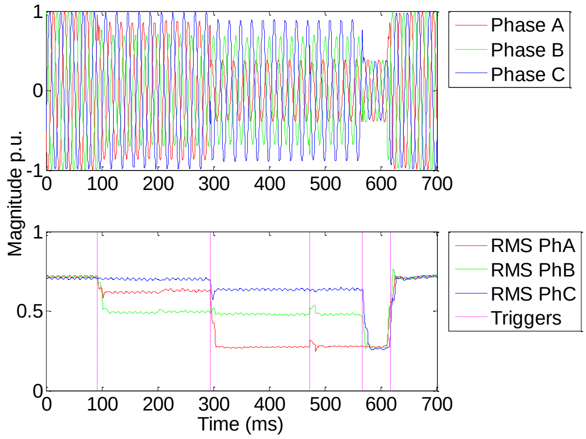

Fig. 9. Multi-stage transition: (a) Voltages waveforms; (b) rms voltages and CaC segmentation.

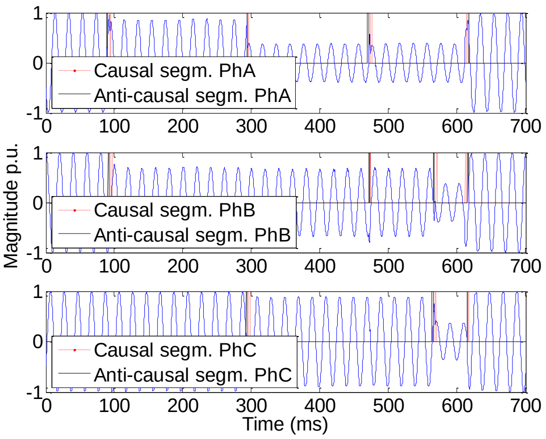

Fig. 10. CaC segmentation for a multi-stage dip.

CONCLUSIONS

Experimental results show that CaC segmentation is useful to detect both slow and fast transitions on recorded dips. The proposed method, based on cusum as statistical estimator and CaC segmentation, accurately detects the transition segments for three phases of different dip types. Furthermore, a classification of dip types can be made based on the proposed method: Dips with fast transition in two phases or fast transition in one phase and no detection in other one, these dips are due to two phases or single phase to ground faults and have a fast recovery; Dips with slow transition on two or three phases, are due to three phases or two phases to ground faults and have a slow recovery.

Acknowledgments

This research is partially supported by FEDER-INNTERCONECTA project Total Integrated GRid Intelligent System (TIGRIS) ITC-20131002, under contract no. 12013095 and by FEDER-INNTERCONECTA project PV-On Time ITC-20131005, under contract no. 12013096. In addition, this work has been supported by the Spanish Ministry of Economy and Competitiveness under Project TEC2013-47316-C3-1-P.

REFERENCES

[1] A. Moreno-Muñoz, Power Quality. Springer London, 2007, p. 423.

[2] C. J. Mozina, “Interconnection protection of IPP generators at commercial/industrial facilities,” IEEE Trans. Ind. Appl., vol. 37, no. 3, pp. 681–688, 2001.

[3] A. Moreno-Munoz, J. J. G. de-la-Rosa, M. A. Lopez-Rodriguez, J. M. Flores-Arias, F. J. Bellido-Outerino, and M. Ruiz-de-Adana, “Improvement of power quality using distributed generation,” Int. J. Electr. Power Energy Syst., vol. 32, no. 10, pp. 1069–1076, Dec. 2010.

[4] A. Moreno-Munoz, J. . Flores-Arias, A. Gil-de-Castro, and J. J. G. de la Rosa, “Power quality for energy efficient buildings,” in 2009 International Conference on Clean Electrical Power, 2009, pp. 191–195.

[5] M. H. Bollen and I. Gu, Signal Processing of Power Quality Disturbances. Wiley, 2006.

[6] C. D. Le, I. Y. H. Gu, and M. H. J. Bollen, “Joint causal and anti-causal segmentation and location of transitions in power disturbances,” in IEEE PES General Meeting, 2010, pp. 1–6.

[7] D. C. Montgomery, Introduction to Statistical Quality Control. 2008.

[8] I. M. Moreno-Garcia, A. Moreno-Munoz, F. Domingo-Perez, V. Pallares-Lopez, R. J. Real-Calvo, and J. J. Gonzalez-de-la-Rosa, “Intelligent electronic device for Smart Grid: Statistical approach applied to event detection,” in IECON 2012 - 38th Annual Conference on IEEE Industrial Electronics Society, 2012, pp. 5221–5226.

[9] I. M. Moreno-Garcia, A. Moreno-Munoz, F. Domingo-Perez, V. P. Lopez, R. Real-Calvo, and J. J. G. de la Rosa, “Smart Grid Inverter Interface: Statistical approach applied to event detection,” in 2012 IEEE International Workshop on Applied Measurements for Power Systems (AMPS) Proceedings, IEEE, 2012, pp. 1–6.